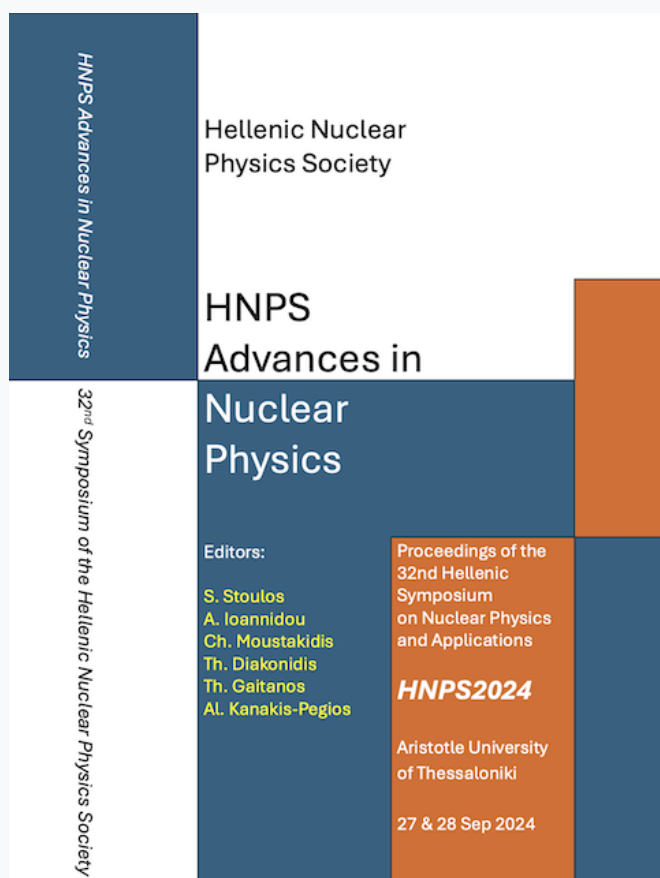


# HNPS Advances in Nuclear Physics

Vol 31 (2025)

HNPS2024



The cover features a blue and orange color scheme. On the left, vertical text reads "HNPS Advances in Nuclear Physics" and "32<sup>nd</sup> Symposium of the Hellenic Nuclear Physics Society". The main title "HNPS Advances in Nuclear Physics" is prominently displayed. Below it, the editors' names are listed: S. Stoulos, A. Ioannidou, Ch. Moustakidis, Th. Diakonidis, Th. Gaitanos, and Al. Kanakis-Pegios. To the right, it specifies "Proceedings of the 32<sup>nd</sup> Hellenic Symposium on Nuclear Physics and Applications", "HNPS2024", and "Aristotle University of Thessaloniki, 27 & 28 Sep 2024".

**Shape coexistence of neutron deficient isotopes near the  $Z = 82$  closure with relativistic energy density functional theory.**

*Konstantinos Karakatsanis*

doi: [10.12681/hnpsanp.8155](https://doi.org/10.12681/hnpsanp.8155)

Copyright © 2025, Konstantinos Karakatsanis



This work is licensed under a [Creative Commons Attribution-NonCommercial-NoDerivatives 4.0](https://creativecommons.org/licenses/by-nc-nd/4.0/).

## To cite this article:

Karakatsanis, K. (2025). Shape coexistence of neutron deficient isotopes near the  $Z = 82$  closure with relativistic energy density functional theory. *HNPS Advances in Nuclear Physics*, 31, 71–78. <https://doi.org/10.12681/hnpsanp.8155>

# Shape coexistence of neutron deficient isotopes near the $Z = 82$ closure with relativistic energy density functional theory.

K.E. Karakatsanis\*

*Department of Electrical & Computer Engineering, Democritus University of Thrace, 67100 Xanthi, Greece*

---

**Abstract** Relativistic energy density functionals have been extensively used to describe shape transitions and coexistence. They provide a consistent framework for studying static and dynamic properties of nuclei across the nuclear chart. Presently, we explore shape coexistence/transitions in the neutron deficient side with  $N=96-112$  around the  $Z = 82$  magic number and in particular for the Hg and Pb isotopes. This area has been extensively researched experimentally, with well-established shape coexistence observed in several isotopes, making it a suitable testing ground for theoretical approaches. Our model is based on the microscopic theory of relativistic energy density functionals. In the first step it involves calculations at the mean-field level, wherein the relativistic Hartree-Bogoliubov equations are solved under constraints on the shape parameters. This enables the construction of potential energy surfaces for the nuclei, revealing the position of the absolute minimum of the ground state and the existence, or absence, of secondary or more minima at different deformations. The second step extends beyond the static mean-field level encompassing the dynamics of rotations and vibrations as collective excitations of the system. The constrained calculations are used to derive mass, inertial parameters and the potential of a five-dimensional collective Hamiltonian (5DCH). Solving the corresponding eigenvalue problem allows for the calculation of excitation energies, of low-lying levels and  $B(E2)$  transition probabilities that can be directly compared with observations. In both steps, we demonstrate how the strength of the pairing interaction affects the theoretical description both quantitatively and qualitatively.

**Keywords** Relativistic mean-field theory, Nuclear structure, Shape coexistence

---

## INTRODUCTION

The study of neutron-deficient Hg and Pb isotopes offers a unique opportunity to explore shape coexistence, a phenomenon where nuclei exhibit multiple configurations with distinct shapes at low energies [1,2]. In the region of neutron numbers  $96 < N < 114$ , these isotopes display a rich variety of shapes, ranging from spherical to oblate and prolate deformations, driven by the interplay between single-particle and collective degrees of freedom. A powerful tool for theoretical investigations of such phenomena is the framework of energy density functionals (EDFs). In this work, we employ the relativistic Hartree-Bogoliubov (RHB) approximation [3,4], based on Lorentz invariant functionals, combined with a finite range pairing interaction, to perform self-consistent mean-field calculations constrained in the quadrupole deformation parameters  $\beta$  and  $\gamma$ . These calculations reveal the evolution of nuclear shapes and the emergence of coexisting minima in the projected energy surfaces (PESs).

To include collective correlations, we construct a quadrupole collective Hamiltonian using parameters derived from the constrained RHB calculations [5]. This allows us to examine low-energy spectra and transition probabilities, providing insights into the collective behavior of these nuclei. Special attention is given to the role of pairing correlations, which significantly influence both ground-state properties and excitation spectra. By adjusting the pairing strength, we aim to improve the theoretical description of shape coexistence and collective dynamics, ensuring better agreement with experimental observations. This study highlights the evolution of nuclear shapes in Hg and Pb

---

\* Corresponding author: kokaraka@physics.duth.gr

isotopes and underscores the importance of pairing correlations in understanding complex nuclear phenomena

## THEORETICAL FRAMEWORK

Energy density functionals are a powerful tool in the theoretical modelling of nuclear structure phenomena. The starting point is an effective interaction between nucleons that defines the form of the energy functional, which in turn depends on the single particle density  $\rho_{nn} = \langle \Phi | c_n^\dagger c_n | \Phi \rangle$  where  $\Phi$  is the ground state wavefunction and  $c_n^\dagger, c_n$  are single nucleon creation and annihilation operators. In the relativistic version a Lorentz covariant interaction is assumed, where nucleons are treated as Dirac spinors, that interact through the exchange of virtual mesons and the electromagnetic field for protons. In addition to the single particle density, it is necessary to include a pairing tensor  $\kappa_{nn} = \langle \Phi | c_n c_n | \Phi \rangle$  since in most nuclei, neutrons and protons fill partially their respective shells. In the end one has the energy functional  $E_{RHB}[\rho, \kappa] = E_{RMF}[\rho] + E_{pair}[\kappa]$ . Variation of  $E$  with respect to the density and pairing tensor leads to the Relativistic Hartree-Bogoliubov (RHB) matrix equation (1):

$$\begin{pmatrix} \hat{h}_D - \lambda & \Delta \\ -\Delta^\dagger & \hat{h}_D^\dagger - \lambda \end{pmatrix} \begin{pmatrix} U_k \\ V_k \end{pmatrix} = E_k \begin{pmatrix} U_k \\ V_k \end{pmatrix} \quad (1)$$

with  $\hat{h}_D = \frac{\delta E}{\delta \rho}$  the Dirac hamiltonian and  $\Delta = \frac{\delta E}{\delta \kappa}$  the pairing gap. This scheme is solved numerically in the mean-field approximation and once the  $U$  and  $V$  Bogoliubov wavefunctions are found, one can in principle calculate any observable of the static ground state of the specific nucleus. Within this framework it is also possible to map the potential energy surface as a function of quadrupole deformation parameters, by solving the RHB equation under constraints on the axial  $\beta$  and triaxial  $\gamma$  degree of freedom.

In order to calculate excitation spectra and transition probabilities of quadrupole vibrations and rotations, we need to include the collective correlations by restoring the symmetries that are broken in the mean-field level. The more formal way is to use the Generator Coordinate Method (GCM) starting from the set of the constrained RHB calculation and projecting the total wavefunction to good quantum numbers. However this is a computationally demanding method especially for heavy nuclei. A similar approach is to use the constrained results for the mapping of the energy surface as input for the construction of a collective Bohr-type Hamiltonian (2):

$$H_{coll} = T_{vib}(\beta, \gamma) + T_{rot}(\beta, \gamma, \Omega) + V_{coll}(\beta, \gamma) \quad (2)$$

The three terms of the hamiltonian are the vibrational kinetic energy  $T_{vib} = \frac{1}{2} B_{\beta\beta} \dot{\beta}^2 + \beta B_{\beta\gamma} \dot{\beta} \dot{\gamma} + \frac{1}{2} \beta^2 B_{\gamma\gamma} \dot{\gamma}^2$ , the rotational kinetic energy  $T_{rot} = \frac{1}{2} \sum_{k=1}^3 I_k \omega_k^2$ , and the collective potential  $V_{coll}(\beta, \gamma) = E_{rot}(\beta, \gamma) - \Delta V_{vib}(\beta, \gamma) - \Delta V_{rot}(\beta, \gamma)$ . The entire dynamics of the collective Hamiltonian is governed by seven functions of the intrinsic deformations  $\beta$ ,  $\gamma$  and  $\Omega$  the three Euler angles: the three mass parameters  $B_{\beta\beta}, B_{\beta\gamma}, B_{\gamma\gamma}$ , the three moments of inertia  $I_k$  and the collective potential. These are all fully determined by the choice of the effective interaction at the starting point of the mean-field calculation.

In this work the parameter sets of DD-ME2 [6] and DD-PC1 [7] have been chosen for the relativistic interaction that takes care of the long-range correlations. For the short-range correlations, the finite range pairing force of Tian, Ma and Ring (TMR) [8] has been selected. This particular force is a modified version of the two body Gogny pairing force, which doesn't require a specific energy cutoff. In coordinate space it has the form  $V(r_1, r_2, r_1', r_2') = -G \delta(R - R') P(r) P(r') \frac{1}{2} (1 - P^\sigma)$ , with  $\mathbf{R}$  the center of mass and  $\mathbf{r}$  the relative distance coordinates. The finite range is given by  $P(r) =$

$\frac{1}{(4\pi a^2)^{3/2}} e^{-r^2/4a^2}$ . The values of the two parameters  $G=728 \text{ MeV fm}^3$  for the strength and  $a=0.644 \text{ fm}$  for the range, have been adjusted to match the pairing gap of the Gogny D1S parametrisation in symmetric nuclear matter. However, in various applications of the described model like the study of rotating nuclei, fission barriers, shape transitions a proper quantitative description is shown to be sensitive to pairing. A common procedure is to readjust the strength parameter using a scaling factor  $f$ . A global analysis of pairing gap calculations across the nuclear chart, using the relativistic functional NL5 [9], has indicated a specific functional dependence of  $f$  on the neutron and or proton number. For those reasons we also examine how pairing adjustment improves our theoretical results using the two functionals DD-PC1 and DD-ME2. More explicitly for each isotope we examine, the scaling factor is chosen as such, so that the calculated neutron and proton pairing gap equals the pairing gap given by the 3-point odd even staggering formula,

$$\Delta_i^3(Q_0) = \frac{\pi Q_0}{2} [B(Q_0 - 1) - 2B(Q_0) + B(Q_0 + 1)] \quad (3)$$

Depending on the isotope, this leads to an increase of about 10-20% in pairing strength.

## RESULTS AND DISCUSSION

### *Mean-field results*

We will first show results obtained by constrained RHB calculations with default and adjusted pairing strength. Since our main objective is to study shape coexistence, we will concentrate our attention at the Projected Energy Surfaces (PES) of each isotope. These are constructed as circular sector diagrams with  $60^\circ$  angle. The radial coordinate represents the  $\beta_2$  quadrupole axial deformation with values from 0 to 0.6. The angular coordinate represents the  $\gamma$  quadrupole triaxial variable with values from  $0^\circ$ , which corresponds to prolate elongation, to  $60^\circ$  which corresponds to oblate elongation. In each separate diagram the global minimum that identifies the shape of the mean-field ground state, is depicted with a red star.

Fig. 1 contains the PES of Hg isotopes with proton number  $Z=80$  and neutrons between  $N=96$ –110, constructed from the RHB calculations with the DD-ME2 interaction and default TMR pairing. Fig. 2 has the same PESs but for TMR pairing adjusted to (3).

The PESs of the Hg isotopes with default TMR exhibit a prolate minimum at approximately  $\beta_2 \sim 0.3$ , which is already present at  $^{176}\text{Hg}$  ( $N=96$ ). This prolate minimum disappears beyond  $^{190}\text{Hg}$  ( $N=110$ ), suggesting that shape coexistence (SC) is expected to occur between neutron numbers  $N=96$  and 110. For the isotopes  $^{184}\text{Hg}$  to  $^{188}\text{Hg}$ , the PESs show increased rigidity in the  $\gamma$  direction, indicating a stronger connection between the prolate and oblate minima. Additionally, the absolute minimum for  $^{190}\text{Hg}$  to  $^{188}\text{Hg}$ , remains on the prolate side, consistent with earlier results obtained using the NL1 parameter set.

In comparison in the adjusted pairing PESs, the appearance of the prolate minimum at  $\beta_2 \sim 0.3$  begins later at  $^{178}\text{Hg}$  ( $N=98$ ) and stops earlier at  $^{188}\text{Hg}$  ( $N=108$ ), limiting the range of shape coexistence to 6 isotopes instead of 8. The PESs of  $^{190}\text{Hg}$  to  $^{188}\text{Hg}$  exhibit greater softness in the  $\gamma$  direction, indicating a weaker connection between the prolate and oblate minima. Additionally, the absolute minimum is better described as being on the oblate side at  $\beta_2 \sim 0.15$ , with only  $^{182}\text{Hg}$  and  $^{184}\text{Hg}$  retaining a prolate absolute minimum. This contrasts with the default pairing results, where the prolate minimum was more persistent across a broader range of isotopes.

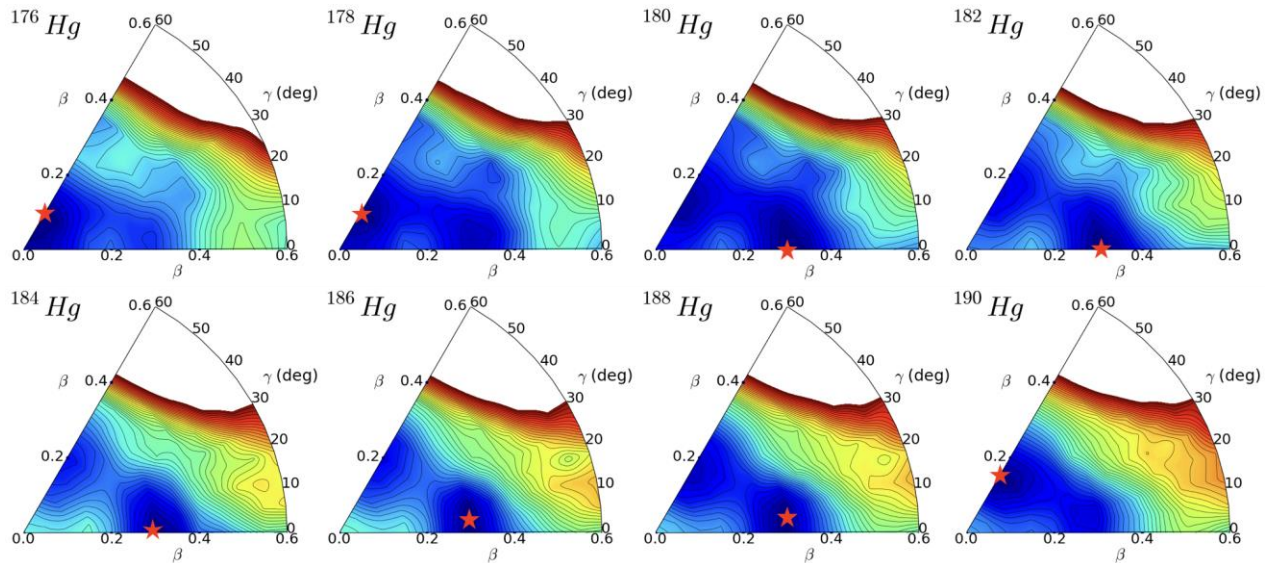


**Figure 1.** PES of even-even isotopes  $^{176-190}\text{Hg}$  using the DD-ME2 interaction and default TMR pairing.

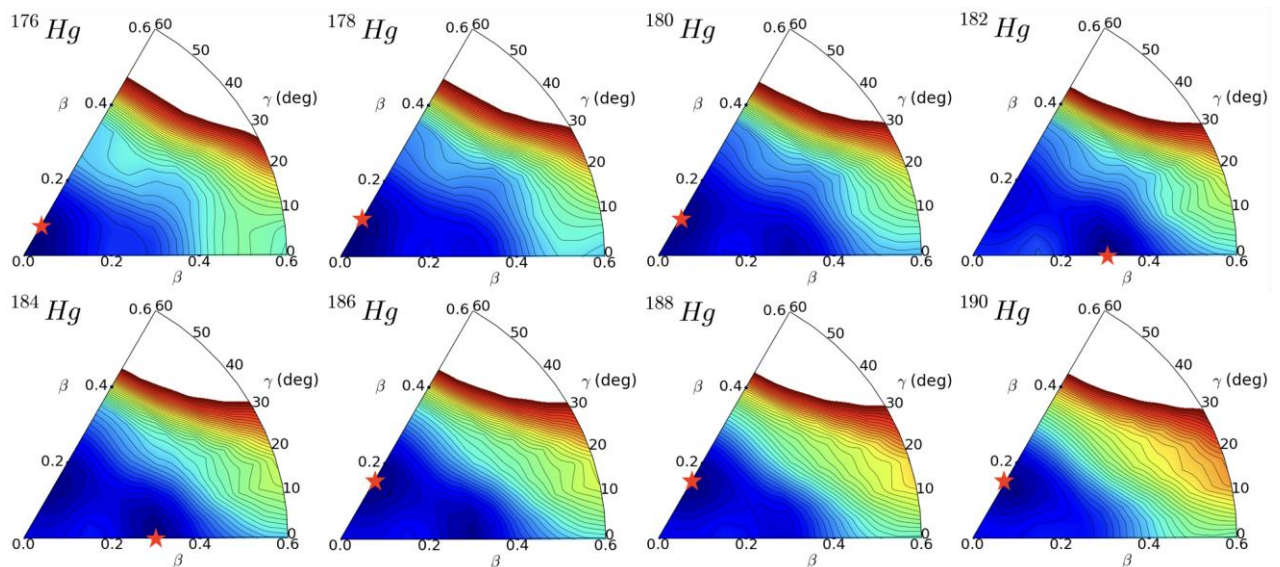


**Figure 2.** Same as Fig. 1, but with adjusted TMR pairing.

The same procedure was applied for Pb isotopes with  $Z = 82$ , which is exactly at the proton shell closure and for the same number of neutrons. Specifically, in Fig. 3 the PESs of  $N=96-110$  Pb isotopes are presented, using the DD-ME2 force and default pairing and figure 4 is the same but with adjusted pairing.

In principle one would expect that all isotopes would acquire a spherical shape. Indeed, a minimum is located at  $(0,0^\circ)$  which is the global minimum for the  $^{178-184}\text{Pb}$  ( $N=96-102$ ) nuclei. In addition to that, two distinct configurations one oblate at  $(0.15,60^\circ)$  and one prolate  $(0.3,0^\circ)$  start to appear at  $^{180}\text{Pb}$  ( $N=98$ ). The prolate minimum becomes very shallow at  $^{186-192}\text{Pb}$  ( $N=110$ ) and it essentially disappears for heavier isotopes. In contrast the oblate minimum becomes dominant, and it is the ground state shape for the isotopes  $^{186-192}\text{Pb}$  ( $N=104-110$ ). For heavier isotopes as we approach the doubly magic isotope  $^{208}\text{Pb}$  the oblate minimum comes closer to the spherical one until they merge. It is important to note that a triple shape coexistence is expected based on these calculations at  $^{182-192}\text{Pb}$  ( $N=98-110$ ).

Comparing Fig. 3 with Fig. 4, the adjusted pairing calculations suggest that the prolate minimum at  $(0.3, 0^\circ)$  appears later in the isotopic chain at  $^{182}\text{Pb}$  ( $N=100$ ) and it has already disappeared at  $^{192}\text{Pb}$  ( $N=110$ ). This means that triple shape coexistence is now limited to  $^{182-190}\text{Pb}$  ( $N=100-108$ ). The shape attribution to the ground state is also different with only  $^{190-192}\text{Pb}$  having an oblate shape, with the rest of the isotopes being spherical.

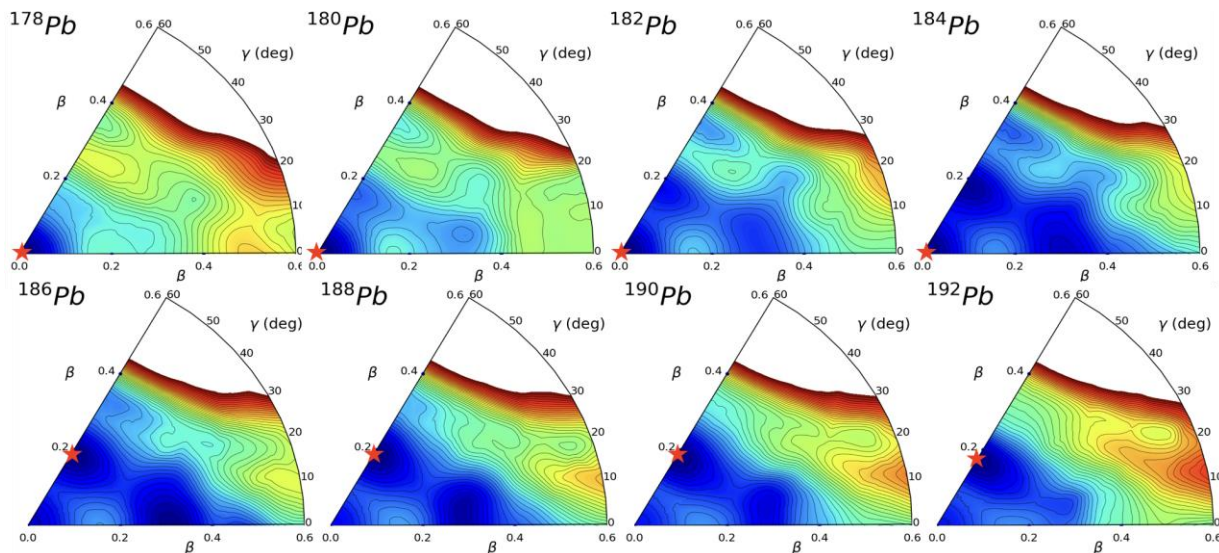


**Figure 3.** PES of even-even isotopes  $^{180-192}\text{Pb}$  using the DD-ME2 interaction and default TMR pairing.

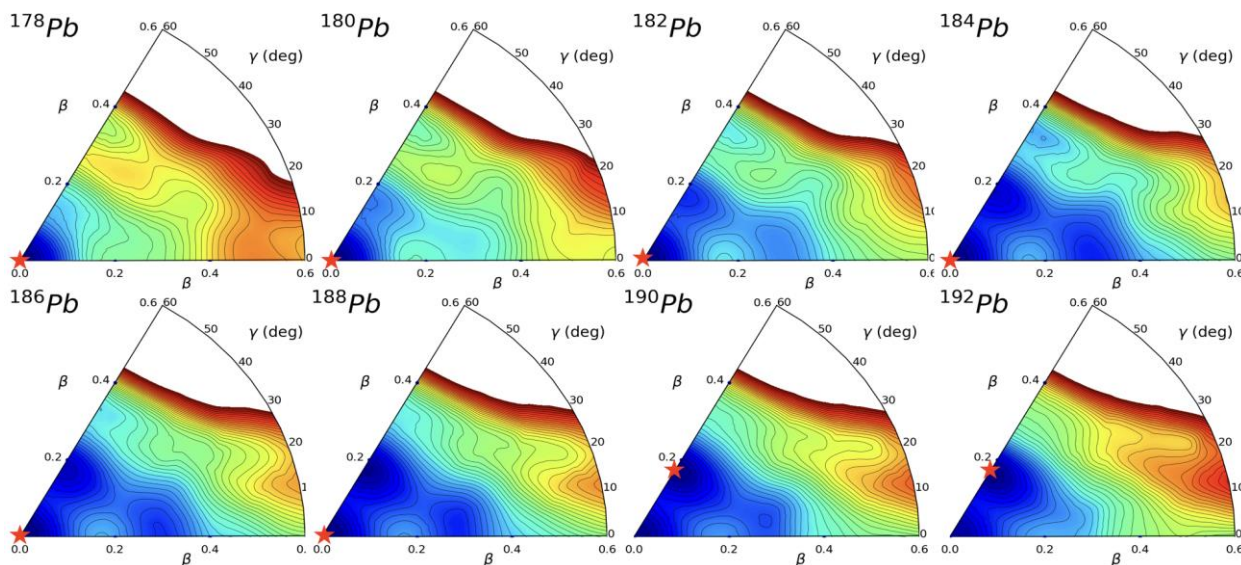


**Figure 4.** Same as Fig. 3, but with adjusted TMR pairing.

### Collective Hamiltonian Results

Evidence of shape coexistence can be found experimentally in the collective spectrum of nuclei. Specifically, the existence of a second collective band of excitation corresponding to a different configuration alongside the ground state band. The position of the low lying states and the band head being close in energy with the levels of the ground state. Increased configuration mixing between the two bands which is measured through the significant value of monopole transition probabilities. It is thus important from a theoretical standpoint to be able to calculate the energies and transition probabilities of the low-lying collective states.

Within our theoretical framework this is done through the collective Hamiltonian, as explained in the previous section. The results of these calculations are shown in the following figures. More specifically, the diagrams in Fig. 5 contain the systematics of the low energy collective states with quantum number up to  $I^\pi = 8^+$ , belonging to the first two bands of the spectrum. With blue dots and continuous lines are the excited states built on the ground state and with red dots and dashed lines are the excited states built on the second configuration. In the left panel we see the states for Hg isotopes with neutron number  $N=96-114$  using the DD-PC1 force. In the right panel we have the Pb isotopes for the same neutron numbers and DD-ME2 force. In both cases the default parameters of TMR pairing were used. Fig. 6 concentrates in the Hg isotopes, showing the systematics of the same states in the left diagram but this time with adjusted pairing parameters and for comparison in the right diagram there are their experimental values. Fig.7 is the same as Fig. 6, but for Pb isotopes.

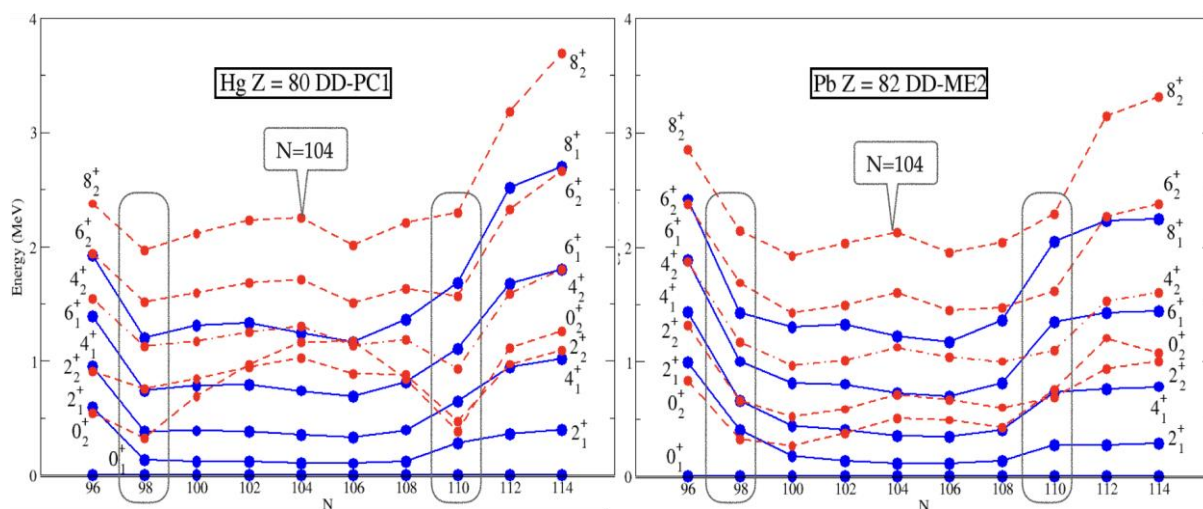


**Figure 5.** Low-lying collective levels systematics for Hg (left panel) and Pb (right panel) isotopes with neutron number  $N=96-114$  and default TMR pairing.

Results with default pairing parameters present a similar pattern of the systematics of their low-lying states for both Hg and Pb isotopic chains. The energies of all levels decrease from  $N=96$  to  $N=98$ . In the region from  $N=98$  to  $N=110$  the excited states of the ground states remain flat, while the energies of the second configuration increase slightly with a peak at the mid-shell  $N=104$  and fluctuate at that energy till  $N=110$ . Beyond  $N=110$  all energies show a rapid increase. The fact that for  $N=98$  and  $N=110$  we get those drastic changes in the systematics is related to the structural changes observed in the PESs of Hg and Pb. Experimentally, this is the neutron region where the characteristic parabolic intrusion of the states of the secondary excited bands takes place (see right panels of Figs. 6 and 7). That is an indication of shape coexistence [1]. The diagrams, however, for the default pairing calculations do not reproduce clearly this feature. In fact, there is the irregular pattern of the secondary excited states that was described with a peak at  $N=104$ , which is pronounced in the case of the  $0_2^+$  state for Hg. In addition, the energy of the first excited  $2_1^+$  state sits far too low in the  $N=98-110$  region.

Adjusting the pairing force at the mean-field level significantly improves the qualitative picture of the systematics. As Fig. 6 shows the calculated excited energies in Hg, follow a parabolic shape for  $N=96$  to  $N=112$ , with a minimum at  $N=104$ , in accordance with the experimental pattern. The position of the first excited  $2_1^+$  also agrees better with the experimental values and  $0_2^+$  has a normalized behavior. An important property that appears within  $N=96-108$ , is the degeneracy between the states of the first and second band that differ by 2 units of total angular momentum i.e. the pairs of states  $4_1^+/2_2^+$ ,  $6_1^+/4_2^+$ ,  $8_1^+/6_2^+$ . One has to note though, that the level density is smaller as compared to both the default pairing calculations and to the experimental data.

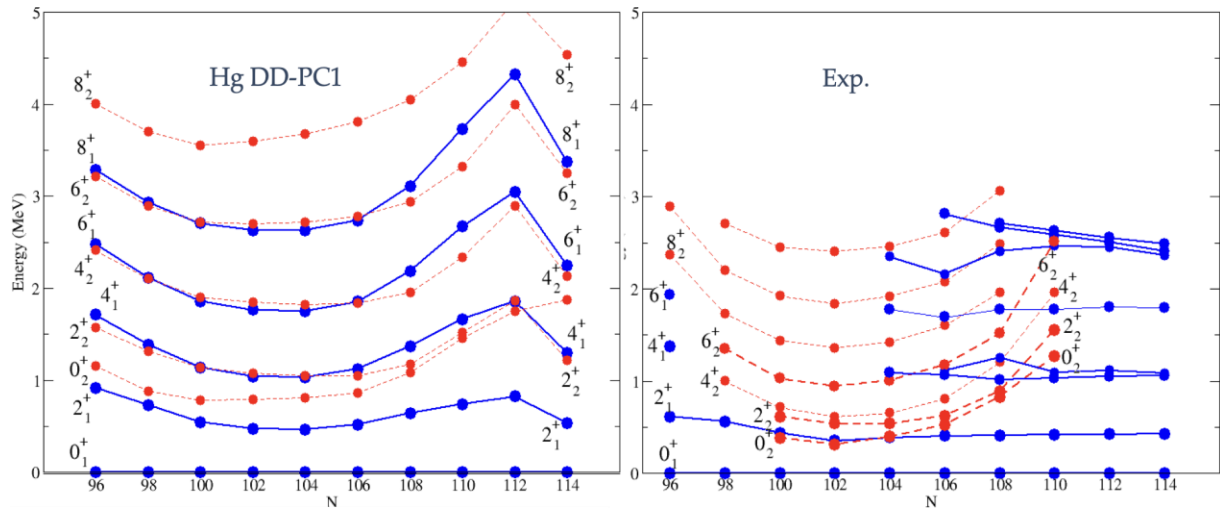


**Figure 6.** Theoretical (left) and experimental (right) low-lying collective levels systematics for Hg with adjusted pairing force.

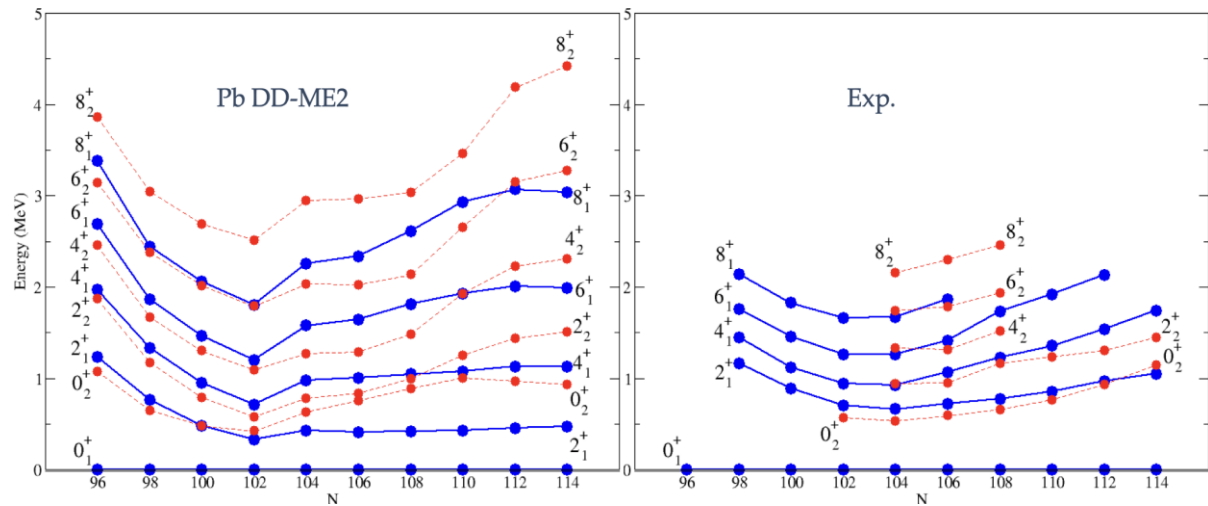


**Figure 7.** Same as Fig. 6, but for Pb isotopes.

The same improvements can be observed for Pb isotopes in Fig. 7. The characteristic parabolic intrusion in the N=96–112 neutrons, is not as smooth and symmetrical as in the Hg case. The position of the first excited  $2^+_1$  follows the experiment until N=104, but then remains constant instead of increasing. Energy degeneracy of the pairs of the states  $2^+_1/0^+_2$ ,  $4^+_1/2^+_2$ ,  $6^+_1/4^+_2$ ,  $8^+_1/2^+_2$  exists in the neutron range N=96–104.

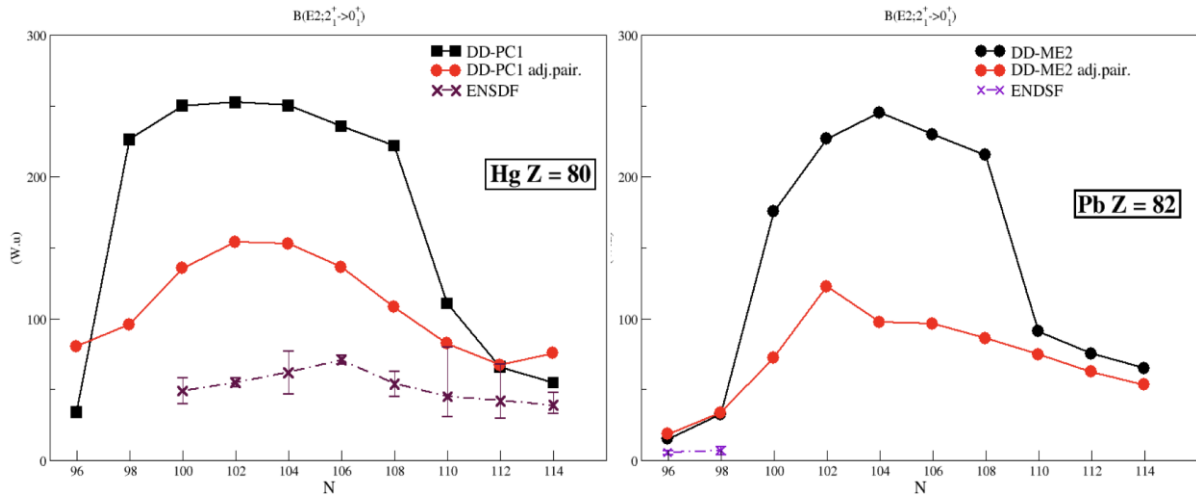


**Figure 8.**  $B(E2; 2^+ \rightarrow 0^+)$  transition probabilities for Hg (left) and Pb (right) isotopes.

Finally, Fig. 8 depicts the behavior of  $B(E2; 2^+ \rightarrow 0^+)$  transition probabilities in Hg and Pb isotopes under default and adjusted pairing schemes. For default pairing, a significant jump is observed at  $N=96$ , followed by a plateau with very large values for  $98 < N < 108$ , indicating excessively strong collectivity. A step down occurs at  $N=110$ , with a gradual decrease toward  $N=114$ . In contrast, adjusted pairing results in a smooth inverted parabolic trend for Hg, with a peak at  $N=102$ , while Pb exhibits a more linear up-and-down curve with the same peak. Both approaches overestimate experimental data for Hg, though the adjusted pairing provides less enhanced  $B(E2)$  values, aligning more closely with experimental observations.

## CONCLUSIONS

Self-consistent mean-field calculations constrained in  $\beta$  and  $\gamma$  deformation were performed for neutron-deficient Hg and Pb isotopes within  $96 < N < 114$ , using the relativistic Hartree-Bogoliubov (RHB) method based on the DD-PC1/DD-ME2 energy density functionals and the TMR pairing interaction. The projected energy surfaces (PESs) reveal a shape evolution from spherical-weakly oblate to coexisting oblate and prolate minima, and back to spherical-weakly oblate for Hg isotopes, while Pb isotopes exhibit triple shape coexistence around the mid-shell at  $N=104$ . A quadrupole collective Hamiltonian, with parameters determined by self-consistent constrained triaxial RHB calculations, was employed to study low-energy spectra and reduced transition probabilities. Adjusting the pairing interaction significantly improves the description at both the mean-field level, by correcting the position of ground-state minima, and beyond mean-field, particularly in reproducing the parabolic pattern of low-lying collective states and the magnitude of  $B(E2)$  transition probabilities.

## References

- [1] K. Heyde and J.L. Wood, *Rev. Mod. Phys.* 83, 1476 (2011); doi: 10.1103/RevModPhys.83.1467
- [2] P. E. Garrett, et. al., *Prog. Part. Nucl. Phys.* 124, 103931 (2022); doi: 10.1016/j.ppnp.2021.103931
- [3] D. Vretenar, et. al., *Phys. Rep.* 409, 101 (2005); doi: 10.1016/j.physrep.2004.10.001
- [4] T. Nikšić, et. al., *Prog. Part. Nucl. Phys.* 66, 519 (2011); doi: 10.1016/j.ppnp.2011.01.055
- [5] T. Nikšić, et. al., *Phys. Rev. C* 79 p. 034303 (2009); doi: 10.1103/PhysRevC.79.034303
- [6] G.A. Lalazissis, et. al., *Phys. Rev. C* 71, p. 024312 (2005); doi: 10.1103/PhysRevC.71.024312
- [7] T. Nikšić, et. al., *Phys. Rev. C* 78, 034318 (2008); doi: 10.1103/PhysRevC.78.034318
- [8] Y. Tian, et. al., *Phys. Lett. B* 676, 44 (2009); doi: 10.1016/j.physletb.2009.04.067
- [9] S. Teeti, et. al., *Phys. Rev. C* 103, 034310 (2021); doi: 10.1103/PhysRevC.103.034310